Hybrid Energy Storage Capacity Optimization Configuration for Wind Power Fluctuation Smoothing Based on GSWOA-VMD

Xuhong Bao*, Bo Zhao and Fang Zhang

Automatization Engineering College, Beijing Information Science & Technology University, Haidian 100192, Beijing, China
E-mail: 2862365747@qq.com
**Corresponding Author*

Received 29 July 2025; Accepted 22 September 2025

Abstract

To reduce the impact of wind power fluctuations on the power grid, this paper proposes a hybrid energy storage system (HESS) capacity optimization configuration method for wind power fluctuation smoothing. The method utilizes a Global Search Whale Optimization Algorithm (GSWOA) to optimize Variational Mode Decomposition (VMD) parameters. First, GSWOA determines the optimal parameter combination (K, α) for VMD. The optimized VMD then decomposes the wind power into a component suitable for direct grid integration and a component requiring smoothing. The smoothing-required component undergoes secondary allocation. Subsequently, an HESS capacity optimization model, considering system costs, is established. This approach achieves efficient wind power fluctuation smoothing and economically optimized operation of the HESS. Case study results demonstrate that

Distributed Generation & Alternative Energy Journal, Vol. 41_1, 167–192.
doi: 10.13052/dgaej2156-3306.4118

the proposed method (GSWOA-VMD) offers superior calculation accuracy and convergence speed compared to alternatives. Furthermore, the HESS configuration exhibits a higher smoothing rate and lower comprehensive cost than single energy storage systems.

Keywords: Global search whale optimization algorithm, variational mode decomposition, wind power fluctuation smoothing, hybrid energy storage, capacity optimization configuration.

1 Introduction

In recent years, the global energy structure has been shifting towards cleaner and low-carbon solutions. Wind energy, as a representative of new energy power generation technologies, has witnessed unprecedented widespread adoption. However, the inherent randomness, intermittency, and volatility of wind power lead to uncertainties in its output. Large-scale direct grid integration increases the regulation burden on power systems, potentially compromising their security, stability, and reliable operation [1, 2]. To effectively address this challenge, this paper proposes a capacity optimization configuration method for Hybrid Energy Storage Systems (HESS) based on the Global Search Whale Optimization Algorithm-optimized Variational Mode Decomposition (GSWOA-VMD). This method adaptively optimizes the parameters of VMD using the Global Search Whale Optimization Algorithm (GSWOA), effectively enhancing the accuracy and efficiency of fluctuating power decomposition, thereby achieving more economical and efficient hybrid energy storage configuration and wind power fluctuation smoothing.

Energy storage technology, with its flexible charging and discharging capabilities, offers an effective solution for smoothing wind power fluctuations, thereby enhancing its grid compatibility. Nevertheless, wind power fluctuations encompass power components with varying frequencies and amplitudes. A single energy storage form often struggles to simultaneously meet multiple requirements such as high energy density, high power density, long lifespan, and fast response. Combining different energy storage technologies allows for the accommodation of distinct fluctuation components [3]. Consequently, Hybrid Energy Storage Systems, leveraging the complementary advantages of diverse storage types, present a superior choice for mitigating wind power fluctuations. Regarding the specific configurations of HESS, existing research has explored various technological pathways such

as flywheel-compressed air [4], pumped hydro-vanadium redox flow battery [5], and superconducting magnetic storage-battery [6], all of which have demonstrated superior performance in mitigating wind power fluctuations compared to single energy storage systems. Among these, the battery-supercapacitor combination [7] has attracted more attention due to its flexible deployment, strong environmental adaptability, mature industrial chain, and potential for large-scale application, alongside the notable complementarity in technical characteristics. Specifically, lithium-ion batteries, as one of the most widely used and promising energy storage technologies, offer high output voltage, broad operating temperature range, high specific capacity, and high charge-discharge efficiency [8]. Supercapacitors, on the other hand, provide high power density, rapid response capability, and long cycle life [9, 10]. The combination of the two effectively handles different components of wind power fluctuations: supercapacitors manage high-frequency and high-power fluctuations, thereby reducing the burden on batteries and extending their service life. This synergy allows the hybrid system to fully exploit its techno-economic advantages. Based on comprehensive considerations of technological maturity, economic feasibility, and complementary characteristics, this paper selects the lithium battery-supercapacitor HESS as the solution for smoothing wind power fluctuations.

The core of this approach lies in decomposing the wind power fluctuation according to frequency characteristics – i.e., separating the original power signal containing broad-frequency fluctuations into sub-components based on frequency and amplitude. Low-frequency, high-energy fluctuations are assigned to energy-type storage units such as lithium batteries, while high-frequency, high-power fluctuations are allocated to power-type storage units like supercapacitors. This frequency-based management strategy helps utilize the strengths of each storage type and optimize overall system performance and economy. However, the effectiveness of this strategy highly depends on the rationality of the power allocation. Inappropriate allocation may not only overload certain storage units and increase operational costs, but also fail to leverage the synergistic potential of the hybrid system, potentially even introducing new fluctuations or reducing smoothing performance [11].

Consequently, achieving efficient and precise decomposition and allocation of fluctuating power remains a pivotal challenge in the application of HESS for wind power fluctuation mitigation. Currently, numerous studies have been conducted by domestic and international scholars. Common power allocation methods include low-pass filtering [12, 13], wavelet decomposition [14, 15], empirical mode decomposition (EMD) [16, 17], and variational

mode decomposition (VMD) [21–23]. Hu et al. [13] employed a first-order low-pass filter to divide wind farm power output signals into high-frequency and low-frequency components, establishing an HESS optimization configuration model that integrates wind power fluctuation smoothing effectiveness, economic benefits from reduced wind curtailment, and total energy storage investment costs. However, the time delay inherent in low-pass filtering may lead to unreasonable power allocation for the energy storage system. Qi et al. [14] utilized wavelet packet decomposition to obtain multi-band components of wind power. From high to low frequency, they sequentially applied local peak shaving and valley filling to each component's time-domain set until the wind power met fluctuation standards, thereby deriving the smoothed grid-integrated power and energy storage power commands. Nevertheless, the effectiveness of wavelet decomposition heavily depends on the selection of the wavelet basis function. Addressing the challenge of smoothing renewable energy fluctuations with HESS, Li et al. [16] proposed an EMD-based capacity optimization configuration model incorporating constraints on the charge/discharge power limits and state-of-charge (SOC) of storage units. However, EMD suffers from mode mixing issues, which adversely affect power allocation performance. The VMD algorithm was proposed by Konstantin et al. in 2014 [18]. During the signal decomposition phase, this algorithm adaptively determines the optimal center frequency and bandwidth for each mode, enabling effective separation of intrinsic mode functions (IMFs) and frequency-domain partitioning of the signal. It overcomes problems such as mode mixing and indistinct frequency features inherent in EMD, possessing a more rigorous mathematical foundation and superior robustness [19, 20]. Wang et al. [21] tackled photovoltaic power fluctuations using VMD to divide the fluctuating power into high- and low-frequency components, subsequently allocating power within an HESS and proposing a VMD-based HESS capacity optimization configuration strategy. Nevertheless, manually setting VMD parameters – the number of modes (K) and the quadratic penalty factor (α) – introduces subjectivity, potentially compromising decomposition performance and consequently affecting subsequent power allocation and system operation effectiveness.

In response to the limitations above, this paper proposes a hybrid energy storage capacity optimization configuration method for smoothing wind power fluctuations based on the GSWOA-VMD. First, the K-means clustering algorithm is applied to raw wind power data to extract typical days characterized by the median fluctuation magnitude. Subsequently, leveraging the powerful global search capability and adaptability of the GSWOA, the

optimal VMD parameter combination (K, α) is determined. This approach overcomes the limitation of subjective parameter setting in traditional methods and enhances the accuracy and rationality of frequency-domain decomposition. Based on the decomposition, and in accordance with national standards for grid-connected wind farm power, the power signal is categorized into a directly grid-integratable component and a component requiring smoothing. The latter undergoes secondary allocation: high-frequency components are assigned to supercapacitors, while low-frequency components are allocated to lithium batteries. Finally, an HESS capacity optimization model is established, considering smoothing effectiveness, storage lifespan degradation, and system costs. This framework achieves efficient mitigation of wind power fluctuations and economically optimized operation of the hybrid energy storage system.

2 Hybrid Energy Storage System for Wind Farms

2.1 Overall Architecture of Wind Power Fluctuation Smoothing System

The structure of the wind farm HESS is illustrated in Figure 1. The system comprises a wind farm, the HESS (consisting of supercapacitors and lithium batteries), and the power grid. The wind farm output power $P_w(t)$ equals the sum of the grid-integrated wind power $P_g(t)$ and the HESS power $P_{hess}(t)$, while $P_{hess}(t)$ is the sum of the lithium battery power $P_b(t)$ and the supercapacitor power $P_{sc}(t)$. The expressions are given by Equations (1) and (2).

$$P_w(t) = P_g(t) + P_{hess}(t) \tag{1}$$

$$P_{hess}(t) = P_b(t) + P_{sc}(t) \tag{2}$$

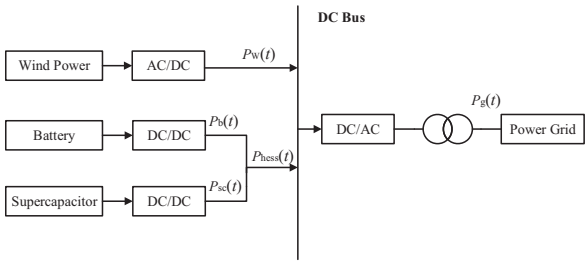

Figure 1 Structure of the wind farm hybrid energy storage system.

Table 1 Maximum permissible rate of change of active power for wind farms Unit: MW

Installed Capacity	Maximum 10-min Variation Power	Maximum 1-min Variation Power
<30	10	3
30–150	Installed Capacity/3	Installed Capacity/10
>150	50	15

In this system, the output power from the wind farm is fed into the DC bus via an AC/DC converter, while the HESS is connected to the same DC bus through bidirectional DC/DC converters, working together to smooth wind power fluctuations. The power allocation commands obtained from the GSWOA-VMD-based decomposition strategy are used to control the lithium battery to absorb/release low-frequency components and the supercapacitor to handle high-frequency components. The charging and discharging behaviors of both storage units are regulated through their respective converters. Finally, the smoothed wind power is integrated into the grid via a DC/AC inverter. From the perspective of practical engineering applications, the coordination and control logic of this architecture can be implemented through a mature Energy Management System (EMS). The EMS issues control commands to the Power Conversion System (PCS) of the hybrid energy storage system based on real-time monitoring of wind power fluctuation characteristics and the status of energy storage devices (such as SOC). The PCS then executes the specific power distribution. This frequency decomposition-based coordinated control strategy not only fully utilizes the technical characteristics of different types of energy storage but also effectively enhances the overall operational economy and reliability of the system, demonstrating strong operational feasibility [24].

2.2 Analysis of National Standards for Wind Farm Grid Integration

To mitigate the impact of large-scale wind power integration on grid operation security, the fluctuation of grid-connected wind power must comply with the Chinese National Standard GB/T 19963–2011 [25]. This standard specifies limits for the magnitude of power change over both 1-minute and 10-minute intervals (as shown in Table 1). These regulations serve as the direct basis for determining the power range that the HESS must smooth, thereby guiding its capacity configuration and power allocation strategy.

3 Hybrid Energy Storage Power Allocation Based on GSWOA-VMD

Prior to the power allocation in the hybrid energy storage system, considering the stochastic nature of wind power output, the K-means algorithm is applied to cluster the raw wind power data (5-minute resolution) to avoid the impact of extreme scenarios, such as prolonged low output or peak values, on the final system capacity configuration and operational strategy. To mitigate the influence of these extreme scenarios and reduce data distortion, a typical day from each cluster was extracted based on the day with the median value of the total fluctuation magnitude within that cluster. The wind power data of these typical days are then adaptively decomposed into K IMFs using the VMD optimized by the GSWOA. Based on the decomposition, and in accordance with the provisions of the Chinese National Standard GB/T 19963-2011 regarding the maximum permissible rate of change of active power for wind farms, the IMF components are classified as follows: The IMFs are cumulatively summed in sequence from low to high frequency to generate a cumulative power series, while calculating in real-time the active power change values of this series over 1-minute and 10-minute time scales. If, upon adding up to the i-th component, its power change value exceeds the limit specified by the standard for the first time, then the first i-1 low-frequency components are classified as the "direct grid integration" part, and the remaining high-frequency components are classified as the "to be smoothed" part. The components requiring smoothing undergo secondary allocation based on frequency characteristics: high-frequency signals are compensated by supercapacitors, and low-frequency signals are compensated by lithium batteries. The resulting grid-connected wind power exhibits effectively reduced fluctuations, meeting the maximum permissible rate of change stipulated by the national standard. The hybrid energy storage power allocation strategy is illustrated in Figure 2.

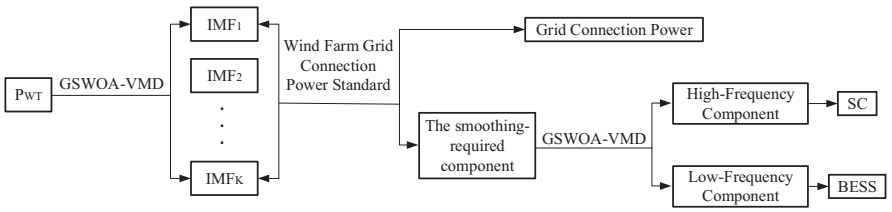

Figure 2 HESS power allocation strategy.

3.1 Variational Mode Decomposition (VMD)

Variational Mode Decomposition (VMD) [26] is an adaptive signal decomposition method. It employs a fully non-recursive variational model that iteratively determines the optimal center frequency and bandwidth for each component. This process adaptively decomposes the signal into k Intrinsic Mode Functions (IMFs), making it suitable for non-stationary and nonlinear signals.

The VMD algorithm decomposes the actual signal f into m IMFs [19], each characterized by its center frequency $\omega(t)$.

The constrained variational model of VMD is represented by Equation (3).

$$\min\left\{\sum_k \left\|\partial_t\left[\left(\delta(t)+\frac{j}{\pi t}\right)*u_k(t)\right]\frac{1}{e^{j\omega_k t}}\right\|_2^2\right\}$$
$$s.t.\sum_{k=1}^{K}u_k=f \tag{3}$$

In Equation (3), $\{u_k\}$ represents the set of K mode functions decomposed by VMD; $\{\omega_k\}$ denotes their respective center frequencies; and $\delta(t)$ is the Dirac delta function.

To solve this constrained optimization problem, a quadratic penalty factor α and an augmented Lagrangian function is introduced as Equation (4).

$$L=\alpha\sum_k\left\|\partial_i\left[\left(\delta(t)+\frac{j}{\pi t}\right)*u_k(t)\right]e^{-j\omega_k t}\right\|_2^2$$
$$+\left\|f(t)-\sum_k u_k(t)\right\|_2^2+\left\langle\lambda(t),f(t)-\sum_k u_k(t)\right\rangle \tag{4}$$

In Equation (4), λ is the Lagrange multiplier; and α is the penalty parameter. VMD utilizes the Alternate Direction Method of Multipliers (ADMM) to find the optimal solution for the constrained variational model, effectively decomposing the actual signal into K IMFs.

3.2 Global Search Whale Optimization Algorithm (GSWOA)

The Whale Optimization Algorithm (WOA), proposed by Seyedali Mirjalili in 2016 [27, 28], is a metaheuristic inspired by humpback whale hunting

behavior. However, it suffers from limitations like weak global search capability and low convergence precision [29]. The GSWOA algorithm addresses these shortcomings by incorporating an adaptive weight mechanism, effectively enhancing convergence speed, search accuracy, and global optimization capability [30]. Its main foraging strategies encompass: encircling prey, spiral bubble-net attacking, and random search. Selection between the first two strategies is based on a random number $r \in (0, 1)$. A non-linearly decreasing inertia weight ω, dynamically adjusted according to the best fitness value encountered by the whale swarm, is represented by Equation (5).

$$\omega(t) = 0.2\cos[\pi/2 \cdot (1 - t/t_{\max})] \tag{5}$$

The specific steps are:

1. Encircling Prey Strategy: When $r < 0.5$, the population adopts the encircling prey strategy. The individual with the highest fitness leads the others in encircling the target.

$$D = |CX^*(t) - X(t)| \tag{6}$$

$$X(t+1) = \omega(t)X^*(t) - AD \tag{7}$$

In Equations (6) and (7), *D* is the distance between other individuals and the best individual; *t* is the current iteration; $X*(t)$ is the position of the best individual at iteration t; $X(t)$ is the position of an individual at iteration t; $X(t+1)$ is the position at iteration $t+1$; A and C are coefficient vectors calculated using Equations (8) and (9).

$$A = 2ar - a \tag{8}$$

$$C = 2r \tag{9}$$

In Equations (8) and (9), r is a random number in (0,1); $a = 2 - 2t/t_{\max}$ (decreasing linearly from 2 to 0 over iterations); $t_{\max}$ is the maximum number of iterations. In this phase, $|A| < 1$.

2. Random Search Strategy: In the random search phase, a random individual is selected as a reference, and others update their positions relative to Equations (10) and (11).

$$D = |CX_{rand}(t) - X(t)| \tag{10}$$

$$X(t+1) = \omega(t)X_{rand}(t) - AD \tag{11}$$

In Equations (10) and (11), $X_{rand}(t)$ is the position of a randomly selected whale. In this phase, $|A| \geq 1$.

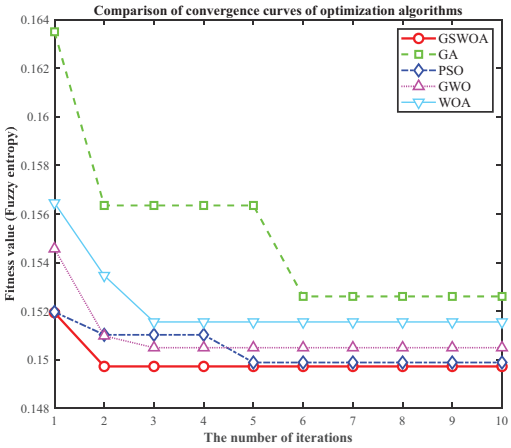

Figure 3 Convergence curves of optimization algorithms.

3. Spiral Bubble-net Attacking Strategy: If $r \geq 0.5$, the whale population approaches the target using a spiral trajectory.

$$D' = |X^*(t) - X(t)| \tag{12}$$

$$X(t+1) = D' e^{bl} \cos(2\pi l) + \omega(t) X^*(t) \tag{13}$$

In Equations (12) and (13), D' is the distance between an individual and the best individual; e is the base of the natural logarithm; b is a constant defining the spiral shape; and l is a random number in $[-1, 1]$.

To validate the optimization performance of GSWOA, VMD parameters were optimized using Genetic Algorithm (GA), Particle Swarm Optimization (PSO), Grey Wolf Optimizer (GWO), standard WOA, and the proposed GSWOA. The convergence curves (fitness value vs. iteration) of these optimization algorithms are shown in Figure 3.

All algorithms were executed on a Windows 11 PC with MATLAB R2024b. As observed in Figure 3, GSWOA converged to its optimal fitness value (0.1497) in merely 2 iterations, demonstrating effective convergence speed. In comparison, GA, PSO, GWO, and WOA converged in 6, 5, 3, and 3 iterations, respectively. Regarding computational time, GSWOA required 169.15 seconds, which is longer than GA (121.57 s) but notably shorter than PSO (429.53 s), GWO (380.59 s), and WOA (568.46 s). This result indicates a favorable balance, as the moderately longer time than GA is offset by improved solution quality and stability, making GSWOA a more efficient choice for this optimization task.

Figure 3 shows that GSWOA demonstrates superior convergence speed and higher optimization accuracy in determining the optimal VMD parameter combination (K, α) compared to GA, PSO, GWO, and the original WOA. Therefore, this paper employs GSWOA to adaptively optimize the key VMD parameters K and α, overcoming the subjectivity limitations of traditional methods and enhancing the precision and effectiveness of subsequent wind power decomposition.

3.3 GSWOA-VMD-Based Hybrid Energy Storage Power Allocation

To determine the optimal VMD parameters and overcome the limitations of traditional optimization algorithms, GSWOA is utilized to optimize VMD parameters, establishing the GSWOA-VMD decomposition method. The flowchart is shown in Figure 4.

The specific steps are:

1. Read typical day data.
2. Initialize GSWOA parameters. Set the search ranges for K and α. Calculate the fitness value for each whale and update positions. Perform

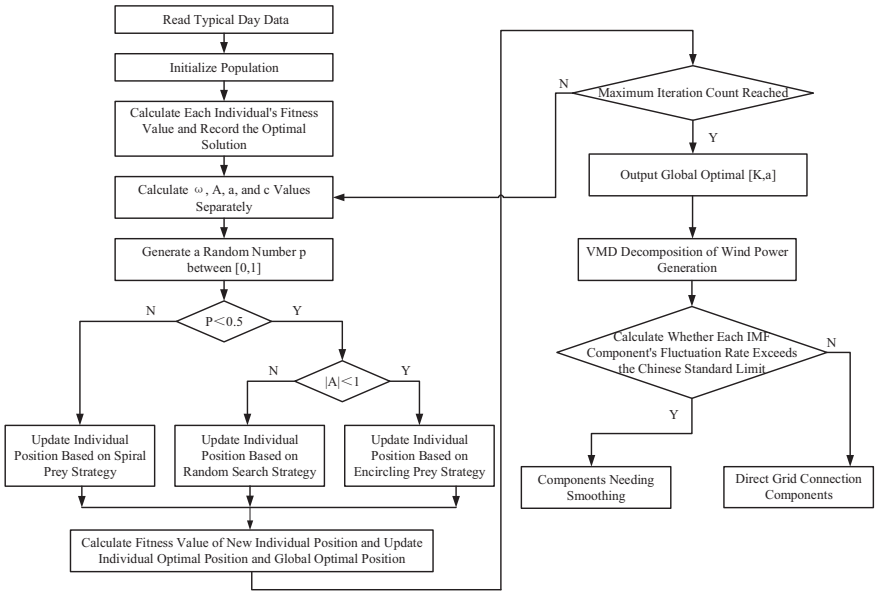

Figure 4 Flowchart of GSWOA-VMD.

contraction-encircling, random search, or spiral updating based on the values of p and $|A|$. Check if the convergence factor a is 0 and if the maximum iteration count is reached. If yes, output the optimal [K, α]; otherwise, continue calculating fitness values and updating positions.

3. Decompose the wind power generation profile (in MW) using VMD with the optimal [K, α], obtaining K IMF components and their frequency spectra. The IMFs retain the original physical units (MW) and are not scaled or normalized, as their absolute magnitudes are directly used for subsequent power allocation and assessment.
4. Calculate the variation rate of each IMF component. Starting from the lowest-frequency IMF, components are sequentially added to reconstruct a partial signal. The fluctuation rate of this cumulative signal is evaluated against the national standard GB/T 19963-2011. Specifically, the 10-minute variation rate is calculated as the maximum difference in power within any rolling 10-minute window. Components satisfying the national standard fluctuation limits are deemed suitable for direct grid integration.

To optimally distribute these smoothing-required components between the supercapacitor (high-frequency) and lithium battery (low-frequency), a frequency boundary must be determined. The initial identification of a candidate boundary (e.g., between IMF4 and IMF5) is guided by the most distinct frequency separation observed in the Hilbert marginal spectrum (Figure 7) [24]. The final selection is validated and determined through a sensitivity analysis, which confirms that this choice leads to the HESS configuration with the lowest comprehensive cost while meeting the smoothing requirement, as detailed in Section 5.3 (Table 5). Following this, the secondary allocation is performed: high-frequency signals from among the smoothing-required components are allocated to the supercapacitor for compensation, while low-frequency signals are assigned to the lithium battery.

To quantitatively evaluate the decomposition performance of VMD with different parameters and to identify the optimal combination [K, α], a fitness function must be defined to guide the GSWOA. In this study, the average fuzzy entropy (FuzzyE$\bar{\text{n}}$) of all obtained IMFs is employed as the fitness function to be minimized. Minimizing FuzzyE$\bar{\text{n}}$ promotes the extraction of regular and well-separated modes, which is the primary goal of the decomposition [31]. The performance of the optimized VMD is subsequently validated using a comprehensive set of metrics, including center frequency variance (Var) and average correlation coefficient (ρ), as detailed in Section 3.4.

3.4 Decomposition Performance Evaluation Metrics for GSWOA-VMD

To objectively assess the decomposition performance of the GSWOA-VMD algorithm, three quantitative evaluation metrics are employed:

1. Center Frequency Variance (Var): Reflects the separation degree of modal components in the frequency domain. The center frequency variance Var is calculated using Equation (14).

$$Var = \frac{1}{K}\sum_{k=1}^{K}(\omega_k - \overline{\omega})^2 \tag{14}$$

   In Equation (14), ω_{k} is the center frequency of the k-th mode, and $\overline{\omega}$ is the mean center frequency. A larger Var indicates better frequency separation.
2. Average Correlation Coefficient ($\bar{\mathrm{R}}$): Characterizes the independence between modal components. The average correlation coefficient $\bar{\mathrm{R}}$ is defined as Equation (15).

$$\overline{\rho} = \frac{2}{K(K-1)}\sum_{i=1}^{K-1}\sum_{j=i+1}^{K}|\rho_{ij}| \tag{15}$$

   In Equation (15), ρ_{ij} is the Pearson correlation coefficient between the i-th and j-th modal components. A smaller R^{-} indicates lower correlation and better independence among modes.
3. Average Fuzzy Entropy: Measures the complexity of modal components based on fuzzy set theory. Average Fuzzy Entropy is defined as Equation (16).

$$D_{ij}^{m} = e^{-(d_{ij}^{m}/r)^2} \tag{16}$$

In Equation (16), D_{ij}^{m} is the distance between vectors, and r is the similarity tolerance. A smaller FuzzyEn̄ indicates more regular components and lower mode mixing.

4 Hybrid Energy Storage Capacity Configuration Model

The smoothing-required components obtained from modal decomposition undergo secondary allocation: low-frequency components are fed into the lithium battery system, and high-frequency components into the supercapacitor system. The HESS capacity configuration model is solved with the

objective of minimizing annual system comprehensive cost. Optimal HESS configuration is achieved through iterative solving.

4.1 Objective Function

The installed capacities of various power units within the region required for this study are shown in Table 1, with the unit of installed capacity being MW.

The total annual comprehensive cost minimization is formulated as Equation (17).

$$\min LCC = C_{inv} + C_{om} + C_{penalty} \tag{17}$$

In Equation (17), investment Cost (C_{inv}) is expressed as Equation (18).

1. Investment Cost

The investment cost represents the equivalent annualized investment of the hybrid energy storage system, used to evaluate the initial capital expenditure of the energy storage capacity configuration. The unit is 10^4CNY:

$$C_{inv} = \frac{r(1+r)^n}{(1+r)^n - 1} \cdot c_{inv} \cdot S_{\max} \tag{18}$$

In Equation (18), *r* is the discount rate; *n* is the lifespan (years); c_{inv} is the unit capacity investment cost (unit: 10^4CNY/MWh); and S_{max} is the maximum capacity of the energy storage system (MWh).

2. Operation and Maintenance Cost

The Operation and Maintenance cost reflects the charging/discharging losses and equipment maintenance expenses during system operation. The unit is 10^4CNY:

$$C_{om} = \sum_t \omega_t (c_{ch} E_{ch}(t) + c_{dis} E_{dis}(t)) \cdot \Delta t \tag{19}$$

In Equation (19), c_{ch} and c_{dis} are the charging and discharging cost coefficients (unit: 10^4CNY/MWh), respectively; $E_{ch}(t)$ and $E_{dis}(t)$ denote the charging and discharging energy of the storage in time period t(MWh); ω_t is the typical day weight; and Δt is the time step length (h).

3. Fluctuation Penalty Cost

The fluctuation penalty cost is used to quantify the negative impact of unsmoothed fluctuating power on the grid. The unit is 10^4CNY:

$$C_{penalty} = \gamma \sum_t \omega_t |P_{wave}(t)| \tag{20}$$

In Equation (20), γ is the penalty coefficient (10^4CNY/MW); $P_{wave}(t)$ is the unsmoothed fluctuating power (MW).

4.2 Constraints

1. Power Balance Constraint is represented by Equation (21).

$$P_{wave}(t) = P_{\sup}(t) - (E_{ch}(t) - E_{dis}(t)) \tag{21}$$

In Equation (21), $P_{\sup}(t)$ denotes the smoothing-required power.

2. State of Charge (SOC) Dynamic Equation is formulated as Equation (22):

$$SOC(t) = (1 - \eta_{sd})SOC(t-1) + \frac{\eta_{ch}E_{ch}(t)\Delta t}{S_{\max}} - \frac{E_{dis}(t)\Delta t}{\eta_{dis}S_{\max}} \tag{22}$$

In Equation (22), η_{ch} and η_{dis} are charge/discharge efficiencies; η_{sd} is the self-discharge rate.

3. Operational Boundary Constraints are expressed in Equation (23).

$$\begin{cases} SOC_{\min} \le SOC(t) \le SOC_{\max} \\ 0 \le E_{ch}(t) \le E_{\max} \\ 0 \le E_{dis}(t) \le E_{\max} \\ E_{\max} = 0.5S_{\max} \end{cases} \tag{23}$$

4.3 Dynamic Baseline Optimization Strategy

Traditional smoothing models aim to eliminate power fluctuations completely by enforcing the grid-integration power to strictly equal the low-frequency component. However, this approach faces challenges in mitigating negative fluctuations (power deficits) due to energy storage limitations, particularly the depth-of-discharge (DOD) and capacity constraints. To address the power allocation and economic optimization problem in the collaborative smoothing of wind power fluctuations with a hybrid energy storage system, this paper proposes a dynamic baseline adjustment mechanism. This strategy reconstructs the smoothing target by introducing a baseline offset δ, as shown in Equation (24).

$$P_{hess}(t) = P_{\sup}(t) - \delta + P_{res}(t) \tag{24}$$

In Equation (24), $P_{res}(t)$ represents the residual fluctuation after smoothing.

The offset δ is treated as a decision variable. Under the premise of meeting grid fluctuation standards, it is incorporated into the overall capacity optimization model for co-optimization. The value of δ is constrained between the minimum and maximum values of the power requiring smoothing, $P_{\sup}(t)$. The global objective of this optimization model is to minimize the total annual comprehensive cost of the system. The solver (CPLEX) automatically searches for the optimal HESS configuration (capacity and power), its charging/discharging strategy, and simultaneously determines the optimal value of δ that leads to the lowest total cost.

The optimal δ value is determined through this global optimization, and its impact mechanism is as follows:

When $\delta < 0$: It means the power reference baseline is adjusted downward. This guides the optimization model to relatively reduce the demand for discharge power from the energy storage system when smoothing negative fluctuations (power deficits), which helps alleviate the deep discharge stress on lithium batteries and prolong their cycle life.

When $\delta > 0$: It means the power reference baseline is adjusted upward. This guides the optimization model to utilize the discharge power of the energy storage system more fully to compensate for power deficits. Given the advantages of supercapacitors in high-rate discharge longevity and economics, the optimization results typically manifest as a more efficient utilization of their discharge capability.

5 Results

5.1 Data and Scenario Construction

To validate the proposed model, real-world data from a 43.2 MW wind farm in Jiangsu, China (5-min resolution, 105,120 points) is used. Typical days are extracted via K-means clustering (k=8 clusters) to capture stochastic wind characteristics. The median-fluctuation sample from each cluster is selected to avoid extreme conditions. Figure 5 shows the power curves of these eight typical days.

5.2 GSWOA-VMD Decomposition Performance

Optimized VMD parameters [K, α] = [8, 2764] (Stage 1) and [8, 2898] (Stage 2) are obtained. Figure 6 displays the time-domain waveforms of the eight IMFs after decomposition. Their Hilbert marginal spectra (Figure 7)

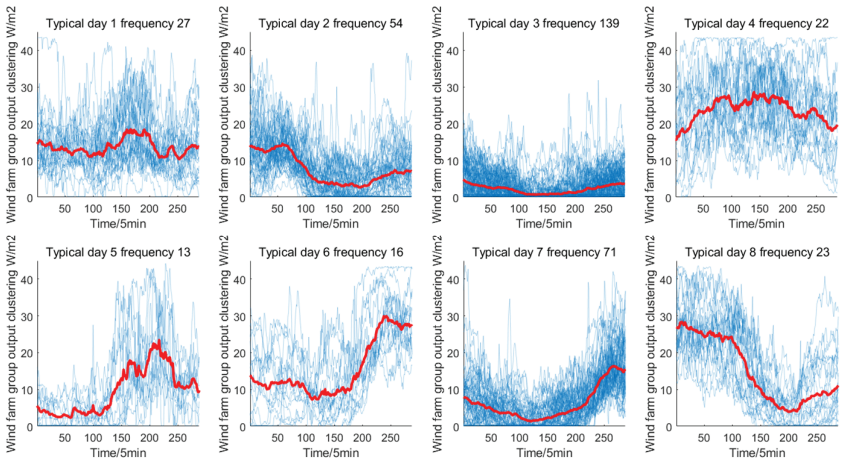

Figure 5 Eight typical daily wind power curves generated by clustering.

Table 2 Comparison of GSWOA-VMD and VMD decomposition performance

Method	Var	ρ	D_{ij}
GSWOA-VMD	0.0276	0.0314	0.3110
Standard VMD	0.0221	0.0414	0.3224

reveal a distinct frequency separation between IMF4 and IMF5, providing a basis for frequency-based power allocation.

Quantitative evaluation using three metrics (center frequency variance Var, average correlation coefficient ρ, average fuzzy entropy D) demonstrates GSWOA-VMD's superiority over standard VMD (fixed K $= 8$, $\alpha = 2000$), as shown in Table 2.

Results indicate effectively improvements: Var increases by 24.9%, ρ decreases by 24.2%, and D_{ij} reduces by 3.8%, validating the efficacy of parameter optimization.

The practical feasibility of the GSWOA-VMD approach is further supported by its computational performance. As detailed in Section 3.2, the GSWOA optimization process for determining the optimal [K, α] parameter combination converged rapidly, requiring only 2 iterations and approximately 169 seconds of computation time. All simulations were performed in a MATLAB R2024b environment running on a Windows 11 operating system. This computational efficiency, combined with its superior convergence performance compared to other metaheuristic algorithms, demonstrates that the

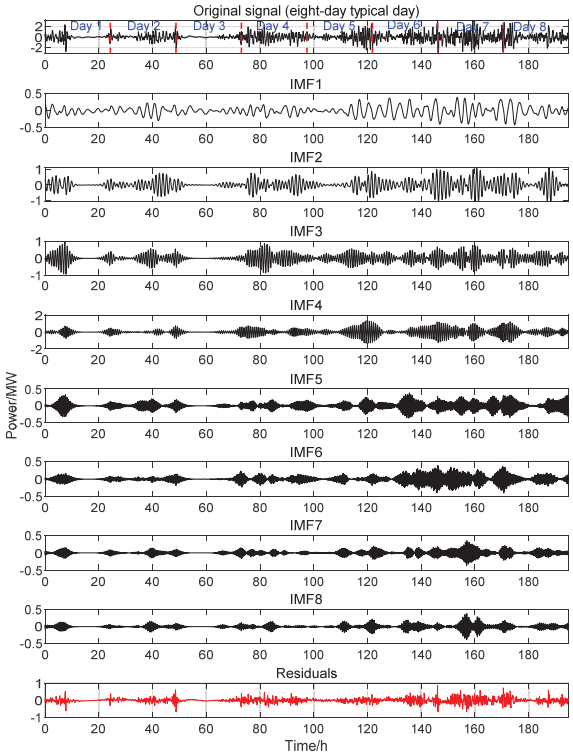

Figure 6 Time-domain decomposition results of the wind power signal using GSWOA-VMD.

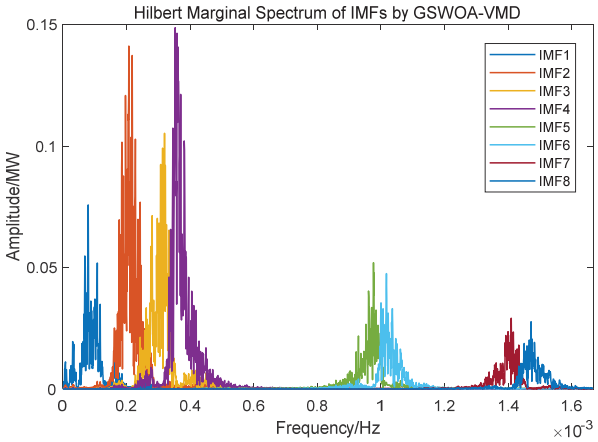

Figure 7 Hilbert marginal spectrum of each IMF component obtained by GSWOA-VMD.

Table 3 Parameters related to hybrid energy storage systems

Parameter	Supercapacitor	Lithium Battery
CAPEX (10^4CNY/(MWh·year))	96.3	–
OPEX (10^4CNY/MWh)	0.001	0.002
C-rate	12C	0.5C
Charge/Dischg Eff.	90%	92%
Self-Discharge Rate	0.005	0.001
SOC Range	10%–90%	20%–90%
Cycle Life	100,000	40,000
Discount Rate	–	8%
Max. DOD	–	80%

Table 4 Optimization configuration results

Parameter	Supercapacitor	Lithium Battery
Capacity (MWh)	0.73	134.55
Max. Power (MW)	8.76	67.28
Baseline Offset (MW)	−0.06	−0.34

proposed method is not only effective but also efficient enough for practical engineering applications, such as the planning and analysis of hybrid energy storage systems.

5.3 HESS Capacity Optimization and Discussion

Based on marginal spectral features, IMF1–IMF4 are allocated to lithium batteries, while IMF5–IMF8 plus residuals are assigned to supercapacitors. The dynamic baseline strategy is implemented to address negative fluctuations. HESS parameters are listed in Table 3, and optimization results in Table 4.

The wind power fluctuation smoothing performance is demonstrated in Figure 8. The upper subplot illustrates the HESS power allocation results, where the low-frequency components assigned to lithium batteries and high-frequency components handled by supercapacitors exhibit distinct time-frequency separation characteristics. The middle subplot compares the original fluctuations requiring smoothing with the HESS-smoothed output, showing effective amplitude attenuation. The lower subplot validates the overall smoothing effect by contrasting the post-processed grid-injection power with the original wind power profile.

To validate the rationality of selecting the IMF4-5 partition point, sensitivity analyses were conducted at three alternative boundaries: IMF3-4, IMF4-5, and IMF5-6. The results are presented in Table 5.

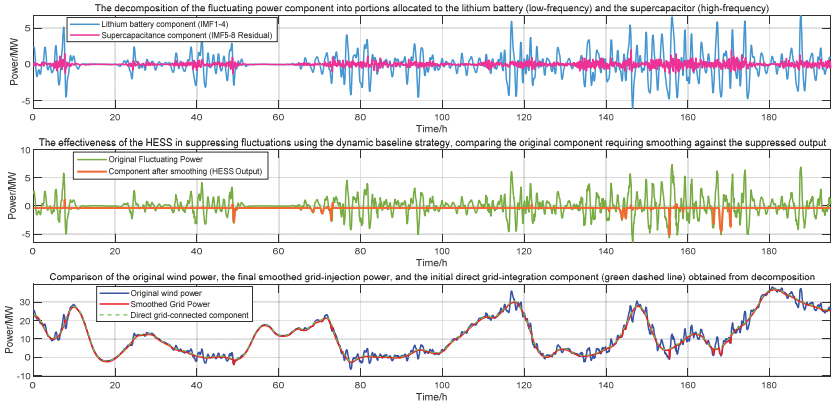

Figure 8 Smoothing performance of the proposed HESS strategy based on GSWOA-VMD and dynamic baseline optimization.

Table 5 Sensitivity analysis of frequency partition points

Partition Point	LiB Cap. (MWh)	SC Cap. (MWh)	Smoothing Rate	Cost (10^4CNY)
IMF3–4	135.29	0.69	83.50%	3116.25
IMF4–5	**134.55**	**0.73**	**83.85%**	**3104.15**
IMF5–6	142.42	0.39	80.40%	3232.07

Results demonstrate that selecting IMF4–5 as the partition point achieves the lowest comprehensive cost (3104.15×10^4CNY) while satisfying fluctuation mitigation requirements (smoothing rate: 83.85%), confirming the economic effectiveness of this partitioning strategy.

The superiority of the IMF4-5 partition can be attributed to the effective alignment between the inherent characteristics of the storage technologies and the frequency-energy properties of the decomposed wind power fluctuations. The Hilbert marginal spectrum (Fig. 7) confirms that modes IMF1-IMF4 primarily consist of low-frequency components with higher energy density, making them suitable for the lithium battery's high-energy-density and slower-response characteristics. In contrast, IMF5-IMF8 contain high-frequency, high-power fluctuations that align perfectly with the supercapacitor's high-power-density and rapid-response capabilities.

From an economic perspective, the sensitivity analysis (Table 5) reveals why alternative partitions are suboptimal. An IMF3-4 boundary assigns an excessive portion of fluctuations to the supercapacitor. Although this further reduces the lithium battery's capacity requirement, the higher unit cost of supercapacitors leads to an increase in the total system

cost (3116.25×10^4CNY). Conversely, an IMF5-6 boundary overloads the lithium battery with mid-to-high-frequency fluctuations, accelerating its degradation and necessitating a larger, more expensive battery configuration to handle the increased power stress, thereby raising the total cost to 3232.07×10^4CNY. Thus, the IMF4-5 partition achieves an optimal techno-economic equilibrium by optimally leveraging the complementary strengths of both storage technologies.

Furthermore, while the specific optimal partition point (e.g., IMF4–5) may vary for different wind farms depending on their unique fluctuation patterns, the overall methodological framework possesses strong generalizability. The GSWOA-VMD algorithm adaptively tunes its parameters (K, α) to capture the local fluctuation characteristics of any given wind power profile. Moreover, the process of identifying candidate boundaries through spectral analysis is universally applicable. This ensures that the proposed method can be effectively deployed to determine a cost-effective storage allocation strategy for diverse wind power integration scenarios.

5.4 Economic Validation of Hybrid Energy Storage

To comparatively analyze the superiority of the hybrid energy storage system, a single storage system (lithium battery only) was optimized as Scheme 1. Scheme 2 employs the proposed HESS (lithium battery + supercapacitor) for wind power fluctuation mitigation. Configuration results are summarized in Table 6.

A comparative analysis reveals several key findings. Scheme 2 achieves enhanced smoothing performance with a 1.97% higher smoothing rate (83.85% vs. 81.88%), primarily due to the supercapacitor's rapid response in compensating for high-frequency fluctuations. Despite the added investment in supercapacitors, there are notable cost reductions. The lithium battery capacity decreases by 10.14% (from 149.71 MWh to 134.55 MWh), and the maximum charge/discharge power reduces by 10.13% (from 74.86 MW

Table 6 Scheme 1 and 2 configuration results

	Scheme 1 (LiB Only)	Scheme 2 (HESS)	
Parameter	LiB	LiB	SC
Capacity (MWh)	149.71	134.55	0.73
Max. Power (MW)	74.86	67.28	8.76
Smoothing Rate (%)	81.88	**83.85**	
Total Cost (10^4CNY)	3346.96	**3104.15**	

to 67.28 MW). Overall, the total cost declines by 7.26%, resulting in a saving of 2.428 million CNY. This outcome demonstrates the synergistic mechanism of the Hybrid Energy Storage System. The supercapacitor efficiently mitigates high-frequency fluctuations, thereby reducing the power variation rate that the lithium battery must handle. Consequently, lithium battery capacity requirements diminish, extending its operational lifespan. Although integrating supercapacitors increases the initial investment, their high-efficiency handling of high-frequency fluctuations optimizes the overall system costs.

In summary, HESS leverages complementary storage characteristics to achieve a superior economic configuration while ensuring effective smoothing performance. This validates its rationality and advantages for applications in wind power fluctuation mitigation.

6 Conclusion

In addressing the issue of hybrid energy storage for smoothing wind power fluctuations, this paper proposes an optimal capacity configuration method for hybrid energy storage based on GSWOA-VMD. Simulation verification is conducted using actual typical day data, leading to the following conclusions:

(1) By optimizing the VMD algorithm with GSWOA, the optimal parameter combination (K $= 8$, $\alpha = 2764/2898$) is obtained, solving the problem of adaptive optimization of VMD parameters. Compared to algorithms such as PSO and GWO, the GSWOA algorithm demonstrates superior computational accuracy and convergence speed.

(2) After decomposing and reconstructing the reference power of hybrid energy storage using GSWOA-VMD, the VMD decomposition performance is effectively optimized (with a 24.9% increase in central frequency variance, a 24.2% reduction in modal correlation coefficient, and a 3.8% reduction in fuzzy entropy). This achieves complementary advantages between lithium batteries and supercapacitors, laying the foundation for the power command division in hybrid energy storage.

(3) Based on the GSWOA-VMD algorithm for smoothing and capacity optimization configuration of hybrid energy storage wind power fluctuations, compared to a single lithium battery, this method increases the smoothing rate from 81.88% to 83.85%, an improvement of 1.97%. It reduces the comprehensive energy storage cost from 33.4696 million CNY to 31.0415 million CNY, a reduction of 7.26%, effectively smoothing wind power fluctuations and achieving economic optimization.

The core framework of the proposed method is generalizable and can provide a reference for addressing the energy storage smoothing problems of other volatile renewable energy sources, such as photovoltaic generation. Regarding implementation feasibility, the optimization results of this paper may serve as a reference for the strategy design of EMS, and the established cost model can also provide an analytical basis for economic evaluation. Future work will focus on promoting the practical application of this method, including researching robust strategies to cope with forecasting uncertainties, validating real-time control performance, and investigating its feasibility and effectiveness in complex scenarios such as multi-site aggregation.

References

[1] Guo Z, Cai Y, Huang S, et al. Research on electricity balance and measurement optimization of new energy power system considering renewable energy consumption mechanism[J]. Distributed Generation and Alternative Energy Journal, 2024, 39(03):483–506.

[2] Liu Z. Long-term Wind power optimization with DQN[J]. Distributed Generation and Alternative Energy Journal, 2025,40(02): 307–332.

[3] Ma L, Xie L R, Ye L, et al. Wind power fluctuation suppression strategy based on hybrid energy storage bi-level programming model[J]. Power System Technology, 2022, 46(03):1016–1029.

[4] Zhang Y, Xu Y J, Guo H, et al. A hybrid energy storage system with optimized operating strategy for mitigating wind power fluctuations[J]. Renewable Energy, 2018, 125:121–132.

[5] Li H Z, Sun D Y, Li B K, et al. Collaborative optimization of VRB-PS hybrid energy storage system for large-scale wind power grid integration[J]. Energy, 2023, 265:126292.

[6] Lu Q Y, Yang Y G, Chen J S, et al. Capacity optimization of hybrid energy storage systems for offshore wind power volatility smoothing[J]. Energy Reports, 2023, 9(S7):575–583.

[7] Kumar G V B and Palanisamy K. Ramp-Rate control for mitigation of solar PV fluctuations with hybrid energy storage system[J]. Distributed Generation and Alternative Energy Journal, 2023, 38(03):817–840.

[8] Liu W, Wu H S, He Z C, et al. A multistage current charging method for Li-Ion battery considering balance of internal consumption and charging speed[J].Transactions of China Electrotechnical Society, 2017, 32(09):112–120.

[9] Vlad A, Singh N, Rolland J, et al. Hybrid supercapacitor-battery materials for fast electrochemical charge storage[J]. Scientific Reports, 2014, 4:4315.
[10] Zhang L, Hu X S, Wang Z P, et al. A review of supercapacitor modeling, estimation, and applications: A control/management perspective [J]. Renewable and Sustainable Energy Reviews, 2018, 81:1868–1878.
[11] Hong F, Jia X Y, Liang L, et al. Hierarchical capacity optimization configuration of hybrid energy storage for wind farm frequency support[J]. Proceedings of the CSEE, 2024, 44(14):5596–5607.
[12] Sang B Y, Wang D S, Yang B, et al. Optimal allocation of energy storage system for smoothing the output fluctuations of new energy[J]. Proceedings of the CSEE, 2014, 34(22):3700–3706.
[13] Hu R, Yin S J, Fu Y. Optimal allocation of hybrid energy storage capacity based on power fluctuations and wind curtailment characteristics[J]. Electrical Measurement & Instrumentation, 2017, 54(19):46–53.
[14] Qi X J, Zheng X W, Wang X R, et al. Improved wavelet packet method of smoothing wind power fluctuations baesd on time-frequency analysis[J]. Acta Energiae Solaris Sinica, 2022, 43(07):302–309.
[15] Yi H, Chen H. Energy management of compound power supply based on grey wolf algorithm[J]. Chinese Journal of Ship Research, 2025, 20(03):249–257.
[16] Li X, Zhang J C, Wang N. Capacity configuration strategy for super capacitor-flywheel- battery hybrid energy storage system[J]. Electric Power, 2018, 51(11):117–124.
[17] Jiang X K, Liu C, Zhang X S, et al. Study on strategy for stabilizing wind power fluctuations based on dual energy storage[J]. Electrical Measurement & Instrumentation, 2025, 62(04):19–25.
[18] Dragomiretskiy K, Zosso D. Variational mode decomposition[J]. IEEE Transactions on Signal Processing, 2014, 62(3):531–544.
[19] Xu Z W, Xiang K X, Wang B, et al. Study on PV power prediction based on VMD-IGWO-LSTM[J]. Distributed Generation and Alternative Energy Journal, 2024, 39(03):507–530.
[20] Du J Y, Lei Y, Li Y K, et al. Hybrid energy storage strategy based on parameter optimized variational mode decomposition[J]. Modern Electric Power, 2021, 38(1):51–59.
[21] Li X, Wang J, Qiu Y, et al.Optimal allocation of hybrid energy storage capacity based on variational mode decomposition[J]. Acta Energiae Solaris Sinica, 2022, 43(02):88–96.

[22] Li W G, Jiao P L, Liu X Y, et al. Capacity optimization configuration of energy storage auxiliary traditional unit frequency modulation based on variational mode decomposition[J]. Power System Protection and Control, 2020, 48(06):43–52.

[23] Li Y M, Ding Z M, Yu Y H, et al. Hybrid energy storage power distribution strategy for micro gas turbine power generation system based on variational mode decomposition[J]. Journal of Xi'an Jiaotong University, 2023, 57(10):183–195.

[24] LIU Y B, ZHANG X, KANG Y L, et al. Capacity allocation of hybrid energy storage system for stabilizing wind power fluctuations through twice decomposition[J]. Proceedings of the CSU-EPSA, 2024, 36(09):61–69.

[25] National technical committee for standardization of electricity regulatory, technical rule for connecting wind farm to power system: GB/T 19963-2011[S]. Beijing: General Administration of Quality Supervision, Inspection and Quarantine of the People's Republic of China, 2011.

[26] Gao X Z, Wang L, Tian J, et al. Research on hybrid energy storage power distribution strategy based on parameter optimization variational mode decomposition[J]. Energy Storage Science and Technology, 2022, 11(01):147–155.

[27] Mirjalili S, Lewis A. The whale optimization algorithm[J]. Advances in Engineering Software, 2016, 95(5):51–67.

[28] Xu F H, and Zhang W. Research on the optimal location of urban electric vehicle charging stations based on the whale optimization algorithm in the context of green energy[J]. Distributed Generation and Alternative Energy Journal, 2025, 40(01):193–212.

[29] Liu L, Bai K Q, Dan Z H,et al. Whale optimization algorithm with global search strategy[J]. Journal of Chinese Computer Systems, 2020, 41(09):1820–1825.

[30] Li D R, Xiao P and Zhai R J, et al. Path planning of welding robots based on developed whale optimization algorithm[C]. 2021 6th International Conference on Control, Robotics and Cybernetics (CRC), 2021, 101–105.

[31] Chen W T, Wang W X, Xie H B, et al. Characterization of surface EMG signal based on fuzzy entropy[J]. IEEE Transactions on Neural Systems and Rehabilitation Engineering, 2007, 15(02):266–272.

Biographies

Xuhong Bao (2000.05–), female, is currently pursuing the M.Eng. degree in control science and engineering at the School of Automation, Beijing Information Science & Technology University. Her research focuses on hybrid energy storage optimization for wind power fluctuation smoothing.

Bo Zhao (1977.01–), male, received the Ph.D. degree from China Electric Power Research Institute. He is currently a researcher and professor-level senior engineer at Beijing Information Science and Technology University. His research focuses on new energy and energy storage, as well as intelligent distribution and power consumption technologies.

Fang Zhang (1979.01–), female, received the Ph.D. degree in Electrical Engineering from North China Electric Power University. She is currently an Associate Professor at Beijing Information Science and Technology University, specializing in analysis and control of modern power systems and smart energy systems.